Arsonic Acid Self-Assembled Monolayers Protect Oxide Surfaces from Micronewton Nanomechanical Forces

*Natalie A. LaFranzo and Joshua A. Maurer**

The development of new surface coatings is critical for combating wear and increasing the device lifetime in microelectromechanical systems (MEMS). Here, a class of arsonic acid self-assembled monolayers (SAMs) is reported that form readily on oxide substrates including silicon oxide, borosilicate glass, and titanium oxide. Monolayers are easily prepared using a straightforward soaking technique, which is amenable to large-scale commercial applications. Monolayer formation on borosilicate glass and titanium oxide is characterized using infrared spectroscopy. Monolayers on borosilicate glass, native silicon oxide and titanium oxide are evaluated with contact angle measurements, as well as wear measurements using nanoscratching experiments. On titanium oxide and borosilicate glass, monolayers prepared from hexadecylarsonic acid provide significantly greater surface protection than surfaces reacted under similar conditions with hexadecylphosphonic acid, a common modifying agent for oxide substrates.

1. Introduction

Microelectromechanical (MEMS) and nanoelectromechanical (NEMS) systems have been established as central to the development of new technologies, particularly in the areas of semiconductors and sensing devices.[1] As with any mechanical system, combating the negative effects of friction and adhesion between contact points is imperative. Prevention of wear, as well as long-term lubrication are important for increasing device lifetime. However, these systems cannot make use of conventional lubricants, such as mineral, vegetable or synthetic oils due to the nanometer-scale mechanical contacts of the devices. As a result, new strategies must be developed for device protection that are applicable to large-scale manufacturing of MEMS and NEMS devices. Self-assembled monolayers (SAMs) have been utilized extensively to tailor the surface properties of the substrates to which they are bonded, and have previously been explored as potential coatings for transistors and sensors, as well as lubricants for MEMS and NEMS devices.[2–9]

SAMs formed from alkanethiols on gold surfaces are well-studied and used in a variety of applications.[10,11] However, this system requires that devices be coated with precious metals such as silver or gold, which are soft and conductive materials and are not amenable to mechanical or electronic applications. Phosphonate monolayers have been demonstrated to exhibit polydentate binding to metal oxides, but, their reactivity is slow and special conditions are typically required to obtain complete substrate coverage. Methods for producing well-ordered phosphonate monolayers including aerosol coating, high-temperature annealing, the T-BAG (tethering by aggregation and growth) method, and substrate pretreating have been developed for stable, well-ordered monolayer formation.[12–19] Alternatively, trichlorosilane and triethoxysilane monomers react readily and quickly with a wide variety of substrates. However, these monomers can react with each other giving rise to cross-linking and leading to coating instability.[20,21] This reduces the durability and utility of silane monolayers for device coatings. Furthermore, the high reactivity of trichlorosilanes with themselves and water, causes the synthesis, purification, and shelf-life of this class of monomers to be problematic.

In order to be useful in wide-spread commercial applications, a straight-forward coating methodology that generates robust, stable surface protection is necessary. We have chosen to exploit the chemical similarities between phosphorus and arsenic to demonstrate the first arsonic acid self-assembled monolayer system. Prepared via a straightforward soaking method, arsonic acid monolayers are stable, non-toxic, and have some degree of ordering. Here, we show the formation of monolayers on titanium oxide, native silicon oxide and borosilicate glass. The ability to form monolayers directly on bare glass demonstrates the increased reactivity of the arsonate headgroup compared to the phosphonate headgroup, which is non-reactive towards glass. The surfaces have been characterized as potential MEMS lubricants using nanoscratching measurements to evaluate the nanotribological properties of the hexadecylarsonic acid SAMs on glass, silicon, and titanium oxide substrates compared to bare unfunctionalized substrates and hexadecylphosphonic acid functionalized substrates prepared under the same conditions.

2. Results and Discussion

2.1. Synthesis and Surface Coating

Many methods to synthesize alkyl arsonic acids have been developed, however early methods were tedious and resulted

N. A. LaFranzo, Prof. J. A. Maurer
Washington University in St. Louis
Department of Chemistry
Center for Materials Innovation
One Brookings Drive
Campus Box 1134, Saint Louis, MO 63130, USA
E-mail: maurer@wustl.edu

DOI: 10.1002/adfm.201202566

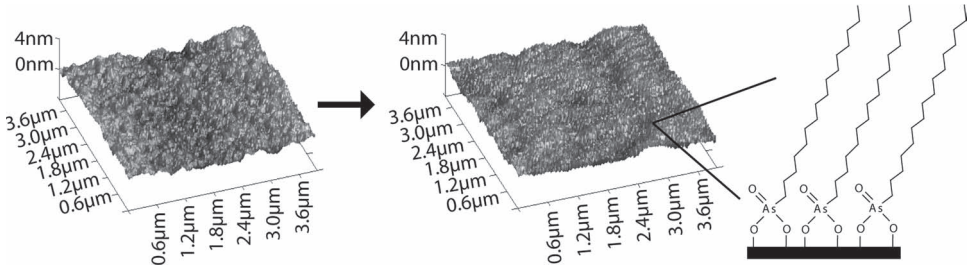

Figure 1. Borosilicate glass substrates are soaked in a 1 mM solution of hexadecylarsonic acid in tetrahydrofuran for 48 h at 40 °C to achieve an arsonic acid self-assembled monolayer (SAM). Height images of functionalized substrates show decreased roughness when analyzed with a 40-nm diamond-tipped cantilever using tapping-mode scanning probe microscopy (SPM).

in a complex mixture of products that were difficult to purify. In 1883, Meyer reported the first synthesis using alkyhalides.[22] This method has become the backbone for modern synthetic methods.[23–25] In 1968, McBrearty and co-workers revisited this work and reported a modified synthetic route that mirrored the synthesis of arsinic acids, using a bis(diethylamin) chloroarsine (BDCA) intermediate.[26] This method is capable of accommodating longer-chain alkyl moieties, up to twenty carbons, with higher purity and yields than previously reported. Since that time, little information on organoarsenic species with high aliphatic character such as these has been reported. Organoarsenic species such as monomethyl and dimethyl arsonic acid, which result from the metabolism of inorganic species, garner much attention due to their toxic nature. However, it is generally regarded that organoarsenic species with large organic groups (either hydrocarbon chains, cyclic moieties, or other functional groups) are excreted from the body, and are therefore less-toxic or nontoxic.[27,28] By simplifying the reaction described by McBrearty and co-workers to a one-pot synthesis, we have streamlined the route to hexadecylarsonic acid. Furthermore, we have found that both in solution and as monolayers hexadecylarsonic acid is not toxic to mammalian cells in culture.

Inspired by the use of phosphonates as coatings for a variety of oxide surfaces,[14,16,18,29] we postulated that arsonic acid molecules would have reactivity towards oxide substrates as well. Slow and limited reactivity is consistently described as a shortcoming of phosphonates that limit their use as coatings for commercial applications. The chemical similarities between arsenic and phosphorus have been described previously,[30] and periodic trends indicate that the arsonic acid headgroup should have higher reactivity. We observe an increased reactivity for hexadecylarsonic acid over hexadecylphosphonic acid that proves to be advantageous and allows for monolayers to be prepared by simpler methods, and on additional substrates.

To develop conditions for arsonate monolayer formation, we evaluated a variety of methods commonly used for phosphonate monolayer formation including T-BAG (tethering by aggregation and growth), slow evaporation, heated soaking, and thermal annealing. To screen these methods, water contact angles were measured following monolayer preparation. In our initial screen, the method that resulted in the highest water contact angle was the heated soaking method, and this method was further optimized as described below.

The simple soaking technique described in **Figure 1** was chosen due to ease and scalability, both of which are imperative for implementation in a commercial manufacturing process. While the technique is time intensive, it does not require significant labor, hands-on processing, or specialized equipment. Furthermore, activated arsonate esters could potentially be employed to reduce the time required for monolayer setting. The substrates used for these experiments are cleaned and further oxidized by oxygen plasma. While this method does not provide a highly-uniform oxide layer, arsonate monolayers form on these substrates. Thus, these monolayers are highly versatile for surface functionalization.[31] As seen in Figure 1, the resulting surface after monolayer assembly is highly uniform. There is no visible "islanding" present on the surface, indicating that the monolayer is formed homogenously on the surface. Markedly, the glass substrate as measured with a diamond-tipped cantilever (40-nm tip radius) using tapping mode AFM, shows decreased roughness following SAM surface preparation. This change in surface roughness may be explained by a difference in nanomechanical properties between the clean, unfunctionalized substrate and the distinctly hydrophobic monolayer, which can affect the interaction of the tip with the surface. To confirm that the reaction of the molecule with the substrate is covalent and results in a well-defined SAM surface, a variety of characterization methods were employed.

2.2. Surface Characterization

2.2.1. Water Contact Angle

Measurement of water contact angle (CA) is one of the simplest methods for characterizing a surface functionalization that results in a change in hydrophobicity. As demonstrated in **Figure 2**, the reaction of hexadecylarsonic acid with borosilicate glass, titanium oxide and silicon oxide all result in water contact angles that on average are greater than 100°. Alternatively, when identical conditions are used to react hexadecylphosphonic acid with these substrates, a water contact angle of greater than 100° is only seen on the titanium oxide substrate. This is not surprising, as phosphonates are known to assemble on titanium oxide, but have not been reported on glass.[14]

To evaluate the differences in CA between a covalently attached SAM and physically adsorbed molecules, arsonate and

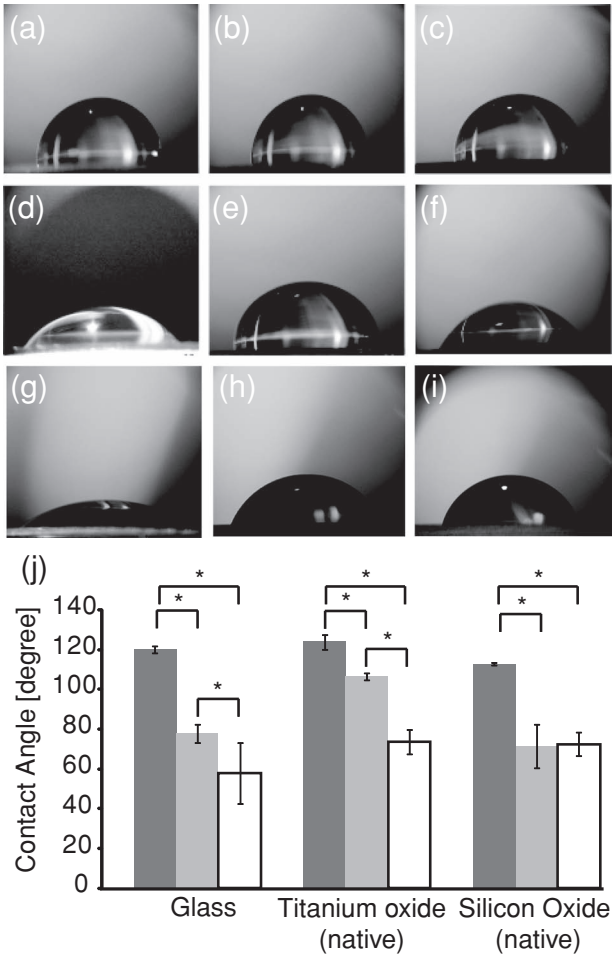

Figure 2. Representative images for water contact angle (CA) measurements for substrates functionalized with arsonic acid and phosphonic acid. Images are arsonate on a) glass, b) titanium oxide, and c) silicon oxide; phosphonate on d) glass, e) titanium oxide, and f) silicon oxide; and pentadecane on g) glass, h) titanium oxide, and i) silicon oxide. Average values for each are summarized in (j). Arsonate monolayers are dark gray bars, phosphonate monolayers are light grey bars, and adsorbed petadecane are white bars. Arsonic acid surfaces have CA values of greater than 100° for all substrates evaluated here, while only phosphonic acid on titanium oxide shows a comparable value. On glass and silicon oxide, the phosphonate surface more closely resembles physisorbed pentadecane. * indicates p value of less than 0.01, n = 6 for all measurements.

phosphonate reacted substrates were compared to substrates soaked in a 1 mM solution of pentadecane, which mirrors the hydrophobic nature of the monomers while lacking a surface reactive headgroup. When compared to these pentadecane-adsorbed substrates, the phosphonate substrates show similar CAs on both glass and silicon oxide. The plot in Figure 2 outlines these differences, and also exhibits that all three arsonic acid SAM substrates are visually and statistically different from pentadecane adsorbed on each.

2.2.2. Infrared Spectroscopy

Fourier-transform infrared spectroscopy (FT-IR) measurements of the arsonate-functionalized titanium oxide and glass substrates were obtained in grazing angle spectral reflectance mode and transmission mode, respectively. **Figure 3** shows representative spectra for each of these samples, and data including errors is contained in Supporting Information Table S1. For our analysis, we define "ordered" monolayers as having asymmetric methylene stretching frequencies below 2920 cm^{-1} and symmetric methylene stretching frequencies below 2850 cm^{-1}. These definitions are based on peak positions for crystalline alkane chains in the extended *trans* conformation.[32] For glass and titanium oxide, we observe that methylene stretching frequencies for the arsonic acid monolayers are very close to those of ordered monolayers. On glass, the average asymmetric stretch is 2920 cm^{-1} and the average symmetric stretch is 2852 cm^{-1}. On titanium oxide, the average asymmetric stretch is 2921 cm^{-1} and the average symmetric stretch is 2852 cm^{-1}. The inability to form "ordered" monolayers based on the classical IR definition is likely due to the size of the arsenic atom in the headgroup of the monomer, which with an atomic radius of 115 pm is larger than the common headgroup atoms of phosphorus and silicon (100 and 110 pm, respectively).[33] This larger headgroup may not allow for tight packing of the monomers on the substrate, thereby introducing the slight disorder observed.

As demonstrated in Figure 3, this method also produces disordered phosphonate monolayers on titanium oxide substrates, with methylene stretching frequencies of 2921 and 2852 cm^{-1}. This is in contrast to other methods that produce highly-ordered phosphonate monolayers. However, titanium oxide substrates prepared by electron beam deposition are rough on the nanometer scale, which may also affect monolayer order and packing. Phosphonate monolayers have not been shown to form on glass substrates, due to a lack of covalent attachment to the surface as described below.

To ensure that the monomers were indeed covalently attached to the substrate, a mechanical peel test was performed.[14,34] Representative FT-IR spectra for the substrates before (dashed lines) and after (solid lines) performing the peel test are presented in Figure 3. There are no significant changes between the two spectra for the arsonic acid monolayers on either substrate or for the phosphonate monolayer on titanium oxide. This indicates that on these substrates a covalent linkage between the monomers and the substrates has been formed. Furthermore, since the intensity does not decrease, the surfaces are likely monolayers and not multilayers. The stark differences in peak positions before and after the peel test for the phosphonate monolayer on glass, as well as the significant decrease in transmission, indicates that the majority of the phosphonate on glass is physisorbed and not covalently attached to the substrate. This is not surprising, as phosphonates are generally regarded as being unreactive towards borosilicate glass.

2.2.3. Mass Spectrometry

Matrix-assisted laser desorption/ionization (MALDI) mass spectrometry has previously been utilized to confirm or identify monolayers assembled on a substrate.[35,36] However, the hydrophobic nature of the arsonic acid substrate is not amenable to consistent, crystalline matrix application for this analysis. As well, the molecular weight of the alkylarsonic acid is found in the same mass range as typical MALDI matrices. Despite these

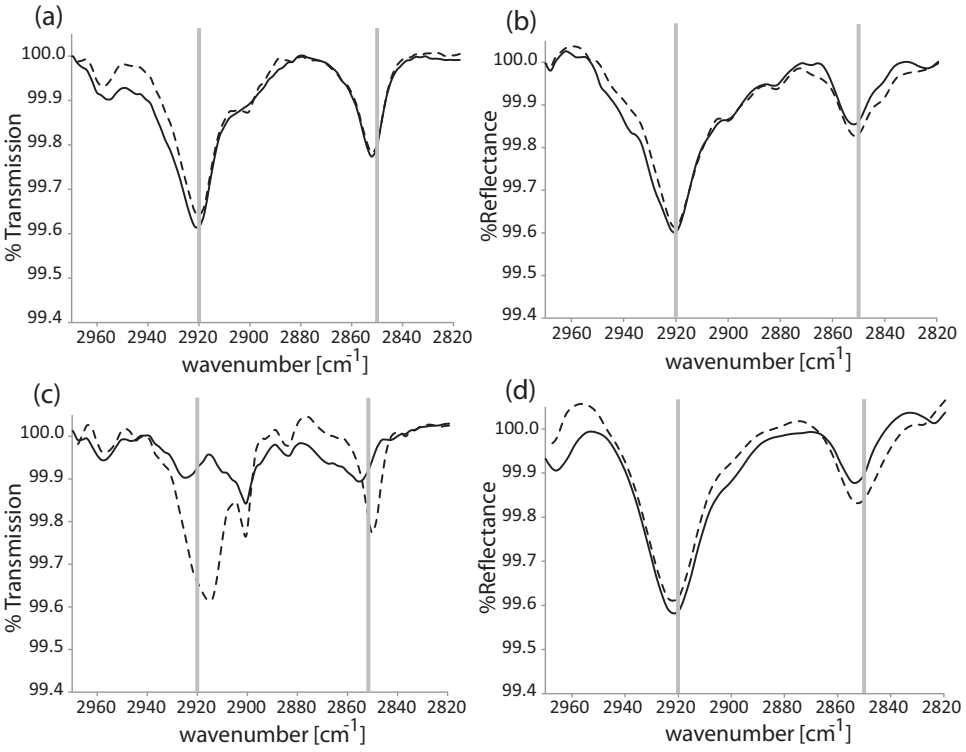

Figure 3. Covalent attachment of monolayers is evaluated using mechanical peel testing and infrared spectroscopy. Representative spectra are shown for a) arsonic acid on glass substrate, b) arsonic acid on titanium oxide substrate, c) phosphonic acid on glass substrate, and d) phosphonic acid on titanium oxide substrate before (dash) and after (solid) the peel test. Grey lines at 2920 and 2850 cm^{-1} indicate asymmetric and symmetric methylene stretches for "ordered" monolayers.

difficulties, MALDI-MS spectra of the arsonate monolayer formed on glass show molecular weight peaks for the $[M+H^+]$ and $[M+Na^+]$ species (see the Supporting Information).

2.3. Nanoscratching

To examine the tribological properties of modified substrates, we utilized a scanning probe microscopy (SPM) based nanoscratching approach. A diamond-tipped cantilever with a nominal tip radius of 40 nm was used to scratch the surface of the substrate at defined forces. Following this wear simulation, the same probe was used to image the scratches on the surface in tapping mode, allowing for measurement of the wear scars. Forces from 22 μN up to 105 μN were evaluated for all substrates. SPM images with 3D renderings of wear scars resulting from application of 88 μN force to the tip during the nanoscratching are shown in **Figure 4**. Bare substrates cleaned by oxygen plasma are compared to those functionalized with hexadecylphosphonic acid and hexadecylarsonic acid. Wear scars on the arsonic acid functionalized substrates are the smallest on all of the substrates. In fact, on titanium oxide there is no visible scarring at these forces. Representative images and raw depth data of the wear scars obtained from each experiment are included in the Supporting Information.

The depths of the wear scars/scratches resulting from these measurements were collected, and the "Percent Protection" was calculated by normalizing the depth of the wear scar on the functionalized substrates by the depth of the wear scar on the corresponding unfunctionalized substrate (**Figure 5**). The arsonic acid monolayers outperform the phosphonic acid coating on both the glass and titanium substrates, showing a greater percent protection at all forces. On the silicon substrates, there is a less visible trend. At lower force regimes (22 and 35 μN), the arsonic acid SAM appears to provide greater protection than the phosphonate coating. However, at higher forces, 53–105 μN, the two coatings appear to perform similarly. This may indicate that the monolayer is not as stable on this substrate as on the other oxide surfaces, and is removed or damaged under the mechanical stress of the scratch. The phosphonic acid and the arsonic acid coating provide significant surface protection over unfunctionalized silicon at these forces. On the titanium oxide surface, the arsonate SAM provides full protection against forces up to 105 μN, which is in stark contrast to the phosphonate monolayer, which only shows moderate protection with significant wear scars above 70 μN.

To further investigate the performance of the arsonic acid SAM on titanium oxide, additional nanoscratches at increased forces ranging from approximately 158 to 263 μN were carried out. The scratch depth data for these measurements are presented, along with the scratch depths observed for lower forces for the unfunctionalized substrate and the arsonate and phosphonate monolayers; see **Figure 6**. Within this greater force regime, wear scars were indeed visible on the substrate, however, the resulting depths are still less than those observed on

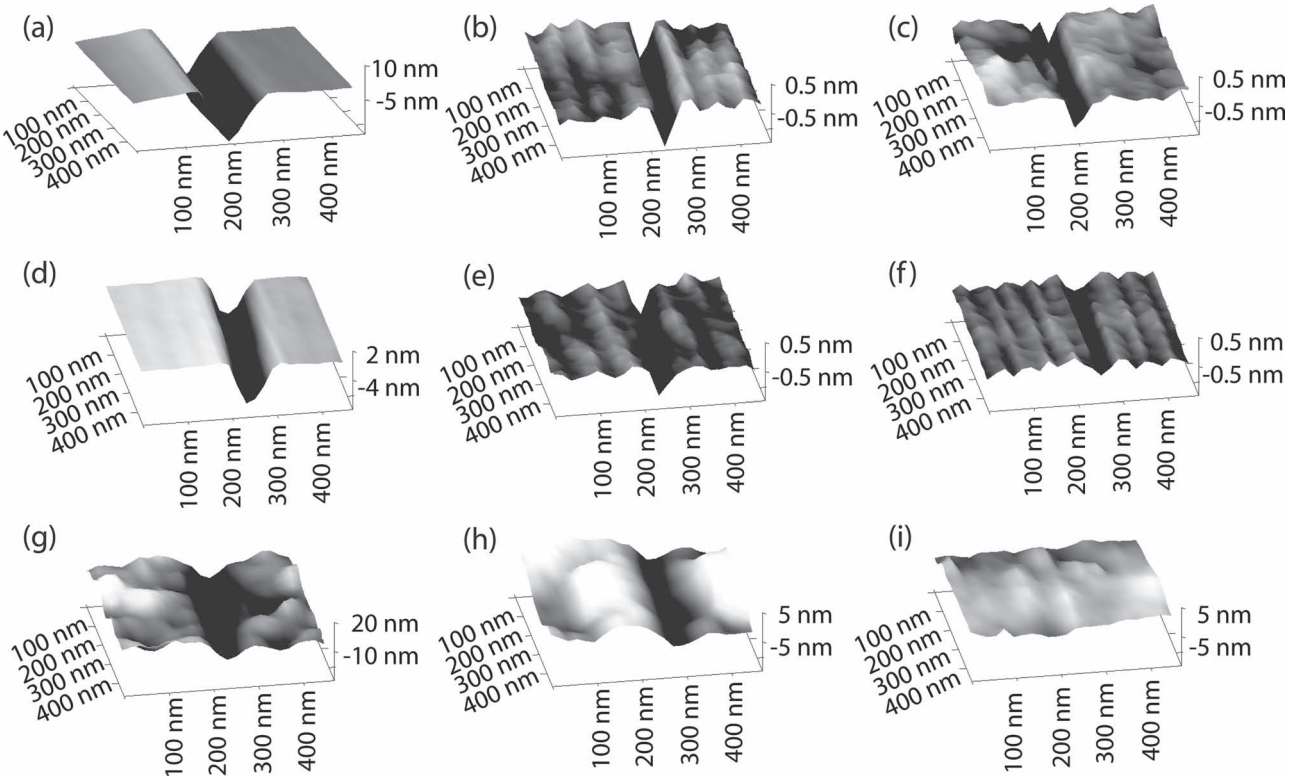

Figure 4. Nanoscratching experiments were used to compare the surface protection abilities of hexadecylarsonic acid to hexadecylphosphonic acid functionalized substrates prepared under identical conditions. The height scale for the images varies to accommodate the scratch depth for each sample. When scratched at a force of 88 μN clear differences between the wear scars are seen. Images (a), (d), and (g) are representative of unfunctionalized borosilicate glass, silicon and titanium oxide substrates, respectively. Images (b), (e), and (h) show the same classes of substrates modified with hexadecylphosphonic acid, and images (c), (f) and (i) are of these substrates modified with hexadecylarsonic acid. Notably, no wear scar is visible on the titanium substrate functionalized with the arsonic acid monolayer (i), while on (g) and (h) these scars are clearly visible despite the increased roughness of the deposited metal oxide.

the unfunctionalized substrate at lower forces. These experiments demonstrate that the arsonic acid SAM coating provides exceptional wear protection on titanium oxide substrates.

3. Conclusions

A one-pot synthesis of hexadecylarsonic acid and a simple method for the preparation of arsonate SAMs on multiple oxide surfaces has been achieved. Additionally, the increased reactivity of arsonates over phosphonates allowed for the functionalization of ordinary glass substrates. The arsonic acid monolayer provides surface protection against micronewton forces on a variety of substrates. As a wear-protection coating, the arsonate monolayer shows better performance on both titanium oxide and glass substrates compared to the corresponding phosphonate analog. As mechanical properties are scale-dependent, the nanoscratching measurement utilized here is particularly relevant to the use of arsonate SAMs as coatings for MEMS devices, where the surface area of the device is large, but the volume is small.[37] The methodology described here is highly facile and amenable to large-scale commercial applications for the functionalization of many oxide substrates, thus it has excellent potential for wear-protection applications within MEMS devices.

4. Experimental Section

Materials: Chemicals were obtained from the following manufacturers and used without further purification: diethyl amine, arsenic trichloride, 1-bromohexadecane, pentadecane and hexadecylphosphonic acid from Sigma-Aldrich; dry tetrahydrofuran (THF) from JT/Mallinckrodt Baker; Magnesium metal turnings from Fisher Sci.; hydrochloric acid (HCl), hydrogen peroxide, dimethylsulfoxide (DMSO) from VWR; diethyl ether from EMD Chemicals; ethanol (100%, absolute) from Pharmco-AAPER; 2,5-dihydroxybenzoic acid (DHB) from TCI America. All reactions were carried out under an argon atmosphere with dry solvents unless noted. Titanium metal and titanium dioxide were obtained from Kurt J. Lesker.

Borosilicate glass coverslips (25 mm, no. 1), were obtained from VWR, International; borosilicate glass slides from SPI Supplies; silicon wafers (2 inch) from University Wafer. Substrates were treated with plasma oxidation before use with a Femto plasma oxidizer (Diener Electronic). Titanium metal and titanium dioxide deposition was performed using a PVD-75 Electron-beam evaporator (Kurt J Lesker).

Instrumentation: ^{1}H NMR and ^{13}C NMR spectra were obtained on a 300 MHz Varian Innova instrument. Electrospray ionization mass spectrometry were obtained on a Thermo LCQ Deca Plus operating in positive mode (ThermoFisher Scientific). Melting point measurements were completed with an Electrothermal Manual Mel-Temp apparatus (Barnstead Thermolyne Corp.). FT-IR spectra were collected on a 670 Nicolet Fourier transform infrared spectrometer with Smart SAGA (spectral apetured grazing angle) reflectance accessory (Thermo Scientific). Matrix-assisted laser desorption/ionization mass

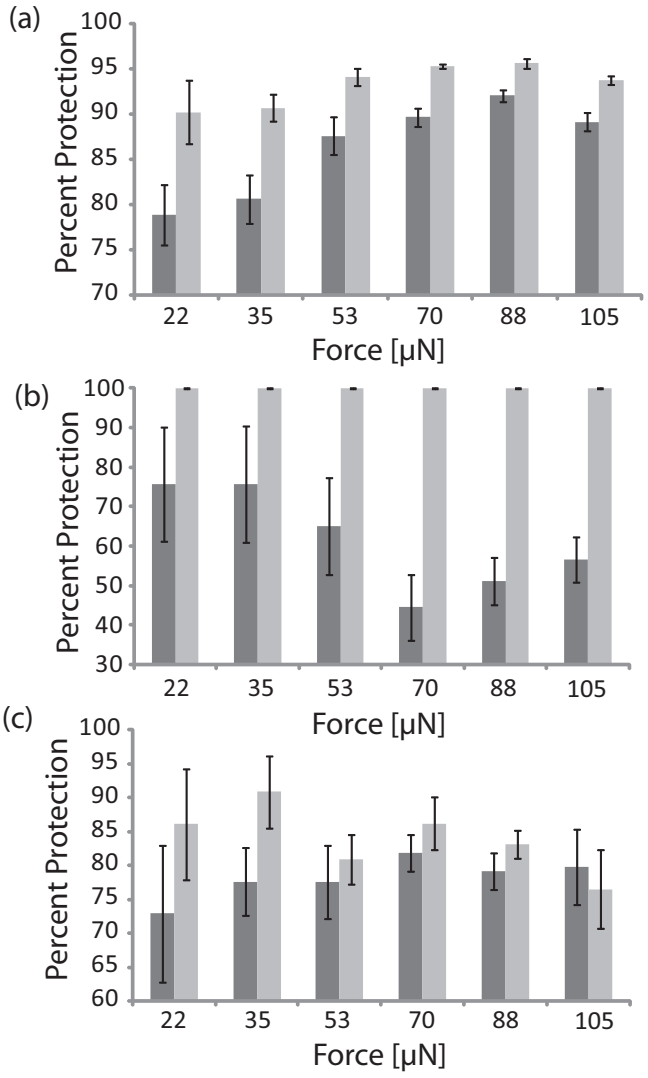

Figure 5. Normalized percent protection compares the wear scars of phosphonate and arsonate functionalized substrates. a) On glass, at all forces, the arsonic acid monolayer protects the substrate from wear better than the phosphonic acid. b) For titanium oxide substrates at the same forces, no wear scars are visible on the arsonic acid substrates, resulting in 100% protection. c) For silicon substrates, at lower forces the arsonic acid surface coating performs better than the phosphonic acid. All measurements are an average of 10 measurements from four different scratches.

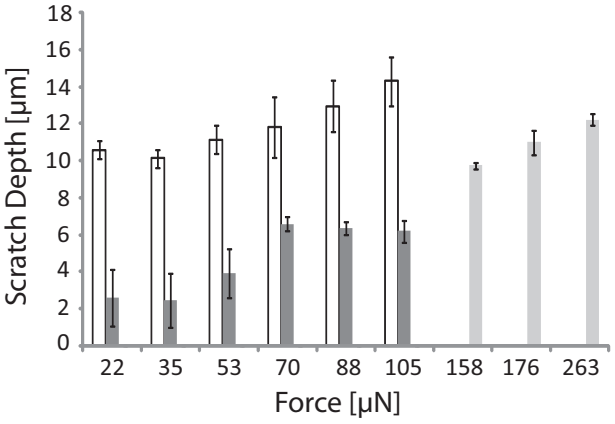

Figure 6. When additional force is applied during nanoscratching experiments on the hexadecylarsonic acid functionalized titanium oxide substrates, wear scars become visible. Unfunctionalized titanium oxide (white bars) are compared to phosphonate (dark grey bars) and arsonate (light grey bars) monolayers on titanium oxide. Arsonate data (light grey bars) from 22 to 105 μN is equal to zero, and is therefore not discernible on the graph. Notably, the scratch depths observed in the higher force regime are lower than those observed for unfunctionalized substrates (white bars) scratched at lower forces. Measurements are an average of ten measurements from four different scratches for all substrates from 22 to 105 μN, and two scratches for arsonate samples within high force regime (158 μN to 263 μN).

spectrometry (MALDI-MS) of the monolayer substrate was obtained on a Voyager-DE STR spectrometer (Applied Biosystems) with 50 shots at an accelerator voltage of 20 000 V and a grid voltage of 96.5%, in positive, linear mode. Contact angle (CA) measurements were made at room temperature using a home-built apparatus consisting of a stage, microscope objective and digital camera. Images were taken with a digital camera and analyzed using the BIGDrop Analysis plugin for ImageJ with the Low Bond Axisymmetric Drop Shape Analysis model.[38] Nanoscratching measurements were obtained on a Multimode VIII scanning probe microscope (SPM) with NanoMan software package (Bruker).

Hexadecylarsonic Acid Monomer Synthesis: Synthesis of 1-hexadecylarsonic acid was based on the method of McBrearty, et al.[26] with modification to a one-pot synthesis as described below. Diethyl amine (3.49 g, 4 eq) was dissolved in THF (20 mL), cooled in a dry ice/acetone bath and arsenic trichloride (1 mL, 1 eq) was added dropwise. The ice bath was removed and reaction was allowed to proceed at room temperature for 3 h. The resulting white precipitate was removed by filtration under argon. Unreacted diethyl amine and solvent were removed from the mixture by distillation at 90 °C. The remaining mixture was added dropwise at 0 °C to a Grignard reagent, prepared from 1-bromohexadecane (2.186 g, 0.6 eq) and magnesium metal turnings (175 mg, 0.6 eq) in THF (20 mL). The reaction was refluxed for 15 hours and then cooled to room temperature. HCl (4 M, 12 mL) was added dropwise and the mixture was refluxed for an additional 1.5 hours. An additional aliquot of HCl (4 M, 10 mL) was added to the flask, and the reaction mixture was extracted with diethyl ether (40 mL) and washed twice with water (20 mL). Hydrogen peroxide (35%, 5.5 mL) was added to the organic layer and the mixture was allowed to stir for 1 h at room temperature. A white solid precipitated out, was filtered and washed twice with ether. The solid was recrystallized from 80% ethanol (200 mL). Yield: 0.860 g (20.4%).

^{1}H NMR (300 MHz, $CDCl_3$ δ): 0.88 (t, 3H); 1.28 (m, 12H); 1.91 (m, 16H); and 2.32 (t, 2H). ^{13}C NMR (300 MHz, $CDCl_3$ δ): 32.15; 29.92; 29.84; 29.74; 29.71; 29.66; 29.64; 29.58; 29.55; 29.41; 29.30; 28.91 22.92; and 14.36. HRMS (ESI, m/z): [M+H$^+$] calcd for $C_{16}H_{36}O_3As$, 351.375, found 350.93. Melting point 122–126 °C.

Surface Preparation: To prepare glass substrates for transmission FT-IR, CA and SPM analysis: borosilicate glass slides and coverslips were cleaned by oxygen plasma at 100% power for 10 min on each side. The slides were subsequently rinsed with ethanol, deionized water, and ethanol, drying with nitrogen gas following each rinse. To prepare titanium substrates for reflectance FT-IR, CA and SPM measurements: borosilicate glass slides and coverslips were cleaned by oxygen plasma at 100% power for 20 min. The slides were subsequently rinsed with ethanol, deionized water, and ethanol, drying with nitrogen gas following each rinse. Titanium (5000 Å) and titanium dioxide (150 Å) were deposited using an electron beam evaporator at a rate of 0.1 Å/s followed by treatment with oxygen plasma at 100% power for 20 min. The slides were

subsequently rinsed with ethanol, deionized water, and ethanol, drying with nitrogen gas following each rinse. To prepare silicon substrates for CA and SPM measurements: silicon wafers were cut to size and cleaned by oxygen plasma using plasma oxidation at 100% power for 20 min. The wafers were subsequently rinsed with ethanol, deionized water, and ethanol, drying with nitrogen gas following each rinse.

Preparation of Self-Assembled Monolayers and Control Surfaces: Substrates were immersed in a 1 mM solution of either hexadecylarsonic acid, hexadecylphosphonic acid or pentadecane in THF and warmed to 40 °C in a jar vented with a small needle to minimize evaporation. Substrates were allowed to soak for 48 h, then rinsed twice with fresh THF for 30 s each, followed by a 1 h soak in THF before rinsing twice with ethanol and drying with nitrogen gas. Substrates were stored dry prior to analysis.

Surface Characterization/Analysis: For contact angle measurements, samples were placed on the stage and a single drop of 18.1 MΩ water was placed on the sample. Drop images were collected and analyzed using the BIGDrop Analysis plugin. For each set of samples, two locations on three different substrates were averaged. Transmission and spectral reflectance infrared spectra and backgrounds were collected as single beam measurements at a resolution of 4 cm^{-1}. Spectra were processed to give percent transmission (%T) or percent reflectance (%R), and baseline corrected. MALDI-MS of monolayer substrates were obtained using DHB matrix dissolved in diethyl ether at 10 mg/mL. MALDI-MS (MALDI-TOF+, *m*/*z*): [*M*+H^+] calcd for $C_{16}H_{36}O_3As$, 351.4, found 351.6. (MALDI-TOF+, *m*/*z*): [*M*+Na^+] calcd for $C_{16}H_{36}O_3As$, 373.4, found 373.2. Mechanical stability of the monolayer was evaluated by the Scotch tape peel test as previously described by Gawalt, et al.[14]

Nanoscratching/Mechanical Wear Testing: Experiments were performed at a temperature of 24–26 °C and a relative humidity of 38–39%. Nanoscratching experiments were executed using a diamond probe on a stainless steel cantilever (MDNISP-HS, nominal tip radius = 40 nm, spring constant = 419 N/m, deflection sensitivity = 419 nm/V, resonant frequency = 66 kHz, Bruker Probes). Scratches were made using NanoMan software in contact mode with a z distance of –20 nm, z-velocity = 50 nm/s, xy-velocity = 1 µm/s with proportional and integral gains of 1.04 and 0.521, respectively. Substrates were scratched with the probe at forces of 21.95, 35.11, 52.67, 70.22, and 105 µN for approximately 5 µm. Surfaces were immediately imaged using tapping mode with the same probe tuned to a drive frequency of 66 kHz. To analyze wear scars, 10 depth slices were analyzed within the same 2 µm region across all samples and scratches. Scratches not visible within the roughness of the sample were considered to have a depth of zero. Samples were scratched in two locations on each sample, and two samples were scratched for each experiment, except for the increased force measurements for arsonate on titanium oxide where two locations on one surface were analyzed.

Supporting Information

Supporting Information is available from the Wiley Online Library or from the author.

Acknowledgements

We would like to thank John Thorton of the Bruker Nano Surfaces Division for his time and invaluable technical support. This work was supported by National Institute of Mental Health (1R01MH085495).

Received: September 6, 2012
Revised: November 7, 2012
Published online: December 6, 2012

[1] N. P. Mahalik, *Int. J. Manuf. Technol. Manag.* **2008**, *13*, 324.
[2] M. de Boer, T. Mayer, *MRS Bull.* **2001**, *26*, 302.
[3] M. Halik, H. Klauk, U. Zschieschang, G. Schmid, C. Dehm, M. Schütz, S. Maisch, F. Effenberger, M. Brunnbauer, F. Stellacci, *Nature* **2004**, *431*, 963.
[4] M. Mottaghi, P. Lang, F. Rodriguez, A. Rumyantseva, A. Yassar, G. Horowitz, S. Lenfant, D. Tondelier, D. Vuillaume, *Adv. Funct. Mater.* **2007**, *17*, 597.
[5] A. Pranzetti, S. Salaun, S. Mieszkin, M. Callow, J. Callow, J. Preece, P. Mendes, *Adv. Funct. Mater.* **2012**, *22*, 3672.
[6] V. Tsukruk, *Adv. Mater.* **2001**, *13*, 95.
[7] S. Patton, K. Eapen, J. Zabinski, J. Sanders, A. Voevodin, *J. Appl. Phys.* **2007**, 102.
[8] M. Halik, A. Hirsch, *Adv. Mater.* **2011**, *23*, 2689.
[9] S. DiBenedetto, A. Facchetti, M. Ratner, T. Marks, *Adv. Mater.* **2009**, *21*, 1407.
[10] J. Love, L. Estroff, J. Kriebel, R. Nuzzo, G. Whitesides, *Chem. Rev.* **2005**, *105*, 1103.
[11] A. Pranzetti, S. Salaün, S. Mieszkin, M. E. Callow, J. A. Callow, J. A. Preece, P. M. Mendes, *Adv. Funct. Mater.* **2012**.
[12] J. Woodward, A. Ulman, D. Schwartz, *Langmuir* **1996**, *12*, 3626.
[13] W. Gao, L. Dickinson, C. Grozinger, F. G. Morin, L. Reven, *Langmuir* **1996**, *12*, 6429.
[14] E. Gawalt, M. Avaltroni, N. Koch, J. Schwartz, *Langmuir* **2001**, *17*, 5736.
[15] P. Thissen, T. Peixoto, R. Longo, W. Peng, W. Schmidt, K. Cho, Y. Chabal, *J. Am. Chem. Soc.* **2012**, *134*, 8869.
[16] M. Dubey, T. Weidner, L. Gamble, D. Castner, *Langmuir* **2010**, *26*, 14747.
[17] E. Hanson, J. Guo, N. Koch, J. Schwartz, S. Bernasek, *J. Am. Chem. Soc.* **2005**, *127*, 10058.
[18] A. Raman, M. Dubey, I. Gouzman, E. S. Gawalt, *Langmuir* **2006**, *22*, 6469.
[19] E. L. Hanson, J. Schwartz, B. Nickel, N. Koch, M. F. Danisman, *J. Am. Chem. Soc.* **2003**, *125*, 16074.
[20] G. Kluth, M. Sung, R. Maboudian, *Langmuir* **1997**, *13*, 3775.
[21] C. A. Schlecht, J. A. Maurer, *RSC Adv.* **2011**, *1*, 1446.
[22] G. Meyer, *Ber. Dtsch. Chem. Ges.* **1883**, *16*, 1439.
[23] A. J. Quick, R. Adams, *J. Am. Chem. Soc* **1922**, *44*, 805.
[24] C. K. Banks, J. F. Morgan, R. L. Clark, E. B. Hatlelid, F. H. Kahler, H. W. Paxton, E. J. Cragoe, R. J. Andres, B. Elpern, R. F. Coles, J. Lawhead, C. S. Hamilton, *J. Am. Chem. Soc.* **1947**, *69*, 927.
[25] K. Irgolic, R. A. Zingaro, M. R. Smith, *J. Organomet. Chem.* **1966**, *6*, 17.
[26] C. F. McBrearty, K. Irgolic, R. A. Zingaro, *J. Organomet. Chem.* **1968**, *12*, 377.
[27] T. Sakurai, C. Kojima, M. Ochiai, T. Ohta, K. Fujiwara, *Int. J. Immunopharmacol.* **2004**, *4*, 179.
[28] S. Adler, L. Haskelberg, F. Bergmann, *J. Chem. Soc.* **1940**, 576.
[29] R. Quiñones, E. S. Gawalt, *Langmuir* **2007**, *23*, 10123.
[30] F. Wolfe-Simon, J. Switzer Blum, T. R. Kulp, G. W. Gordon, S. E. Hoeft, J. Pett-Ridge, J. F. Stolz, S. M. Webb, P. K. Weber, P. C. Davies, A. D. Anbar, R. S. Oremland, *Science* **2011**, *332*, 1163.
[31] M. Shinohara, T. Katagiri, K. Iwatsuji, Y. Matsuda, H. Fujiyama, Y. Kimura, M. Niwano, *Thin Solid Films* **2005**, *475*, 128.
[32] R. G. Snyder, J. H. Schachtschneider, *Spectrochem. Acta* **1963**, *19*, 85.
[33] J. C. Slater, *J. Chem. Phys.* **1964**, *41*, 3199.
[34] *Adhesion Measurement of Thin Films, Thick Films, and Bulk Coatings* (Ed: K. L. Mittal), American Society for Testing and Materials, Philadelphia, PA **1978**.
[35] M. J. Hynes, J. A. Maurer, *Angew. Chem. Int. Ed.* **2012**, *51*, 2151.
[36] M. Mrksich, *ACS Nano* **2008**, *2*, 7.
[37] B. Bhushan, *Philos. Trans.: Math., Phys. Eng. Sci.* **2008**, *366*, 1499.
[38] A. Stalder, G. Kulik, D. Sage, L. Barbieri, P. Hoffmann, *Colloids Surf., A* **2006**, *286*, 92.